



Minimizing power consumption of boil off gas (BOG) recondensation process by power generation using cold energy in liquefied natural gas (LNG) regasification process

Tong Yuan, Chunxiao Song, Junjiang Bao^{*}, Ning Zhang, Xiaopeng Zhang, Gaohong He^{**}

State Key Laboratory of Fine Chemicals, School of Petroleum and Chemical Engineering, Dalian University of Technology, Panjin, 124221, China

ARTICLE INFO

Article history:

Received 28 February 2019

Received in revised form

19 June 2019

Accepted 6 August 2019

Available online 9 August 2019

Handling Editor: Jin-Kuk Kim

Keywords:

BOG recondensation

LNG regasification

Integrated system

Power consumption comparison

ABSTRACT

During the process of storage and transportation of liquefied natural gas (LNG), boil off gas (BOG) is generated. The presence of BOG causes the rise of pressure of the storage tank, and makes the LNG receiving terminal have a large safety hazard, which needs to be condensed and recovered. BOG recondensation process is a high power-consumption process, and meanwhile LNG regasification process releases a large amount of cold energy, which can be used to generate electricity. In order to reduce the power consumption of BOG recondensation process, this paper proposes the idea of power generation using cold energy in LNG regasification process to drive the compressors and LNG pumps in BOG recondensation process. Firstly, the cold energy recovery potentials of four different BOG recondensation processes are determined through parameter analysis and power consumption comparison. Based on this, four BOG recondensation and LNG cold energy power generation integrated systems are proposed, and the parameters and working fluids of the integrated system are optimized. Results show that the power consumptions of the integrated systems are significantly lower than those of the original BOG recondensation systems at different BOG contents. In most cases, the proposed system can meet the power requirement of the BOG recondensation process, and at the same time has the ability to output electrical energy. The power reduction rate of the integrated system decreases as the BOG content increases. When the BOG content is 0.03, the power reduction rate can be up to 250%. When the BOG content is 0.15, the power reduction rate can be up to 120%.

© 2019 Elsevier Ltd. All rights reserved.

1. Introduction

With the development of the world economy, the environmental pollution caused by coal and oil is becoming more and more serious. Many countries urgently seek clean and efficient alternative energy sources (Pio and Salzano, 2019; Shi et al., 2015). Natural gas is a high-quality clean low-carbon energy source that can be positively complemented by renewable energy development (Wu et al., 2019). Therefore, the proportion of natural gas in energy supply is increasing rapidly (Karimi and Khan, 2018).

To facilitate long-distance transportation, after pretreatment (Mallapragada et al., 2018; Pospíšil et al., 2019), the natural gas is liquefied to $-162\text{ }^{\circ}\text{C}$, and the volume becomes 1/600 of the original

volume (Salimpour and Zahedi, 2012). Liquefied natural gas is transported to LNG receiving terminals through LNG ships, and is conveyed to users after regasification in LNG receiving terminals (Atienza-Márquez et al., 2018).

LNG receiving terminal is an important link connecting the gas source and the user in the entire LNG industry chain. At present, there are two main problems in the LNG receiving terminal. The first problem is about BOG management. In the process of storage and unloading of liquefied natural gas, storage tanks and pipelines cannot achieve absolute heat insulation, and inevitably generate BOG (Li and Wen, 2017). If the BOG in the tank is not treated in time, the temperature and pressure of the tank will rise. Excessively high pressure will damage the structure of tank and cause danger (Shin et al., 2007). Therefore, when the pressure in the tank is too high, the safety valve of the system will be opened, and the BOG will be directly discharged into the atmosphere, which will cause direct economic loss and serious environmental pollution (Liu et al., 2010).

^{*} Corresponding author.

^{**} Corresponding author.

E-mail addresses: baojj@dlut.edu.cn (J. Bao), hgaohong@dlut.edu.cn (G. He).

The second problem is the LNG cold energy recovery. Liquefied natural gas needs to be vaporized before being sent to the user. During the vaporization process, LNG will release a large amount of cold energy, which is about 830 kJ/kg (Le et al., 2018). Open rack vaporizers, submerged combustion vaporizers and intermediate fluid vaporizers are used in traditional LNG regasification processes (Agarwal et al., 2017). The cold energy carried by LNG is usually taken away by sea water or air, causing extreme waste of energy and severe cold pollution in the surrounding environment (Song et al., 2017). LNG cold energy is a kind of high-quality clean energy, if it is converted into electric energy with 100% efficiency, which is equivalent to 240 kW h/t of electric energy (Hongtan and Lixin, 1999).

Therefore, the effective recovery and utilization of BOG and cold energy of LNG is of great significance to the full utilization of energy and the alleviation of energy shortages. The management of BOG is currently focused on the study of BOG recondensation process. The BOG recondensation process utilizes LNG cold energy to condense and recover BOG, and then it mainly uses pump to pressurize the LNG to the pipe network pressure (Li and Wen, 2017). Querol et al. (2010) compared and analyzed the performance of BOG direct compression system and recondensation system at different LNG compositions. The results showed that the BOG recondensation was the best choice to expand the BOG processing capacity of the LNG receiving terminal. Liu et al. (2010) used the system's power consumption as an objective function to explore the optimal number of stages of compression using the superstructure in BOG recondensation process. It was concluded that when the compression stages were four, the system had the lowest power consumption. In order to reduce the power consumption of the recondensation system, Li et al. (2012) proposed a recondensation system that used high pressure LNG to cool the inlet temperature of the recondenser. Then they proposed the concept of two-stage recondensation, which further reduce the energy consumption (Li and Wen, 2017). Rao et al. (2016) improved the structure of traditional BOG recondensation and analyzed the power consumption of nine BOG recondensation systems. It was concluded that the BOG two-stage recondensation system had the lowest power consumption when the BOG content was 0.15, and the power consumption was reduced by 18.77% compared with the indirect-contact type BOG recondensation system. In the subsequent work, they proved that the BOG two-stage recondensation system was superior to the one-stage recondensation system at different BOG contents (Nagesh Rao and Karimi, 2018).

For cold energy waste for LNG receiving terminal, due to the temperature range of LNG regasification process is large, its cold energy can be applied to crushed rubber, cold energy generation (Kanbur et al., 2018; Tomkow and Cholewinski, 2015), high-purity ozone production, air liquefaction separation (Mehrpooya et al., 2017), dry ice manufacturing (Tuinier et al., 2010), seawater desalination (Williams et al., 2015), food freezing (Messineo and Panno, 2008) and so on. Among them, when cold energy is recovered in the form of electric energy, its industrial chain is short, less interfered by external factors, and has little impact on the environment. Therefore, it has received extensive researches and attentions. LNG cold energy power generation technologies (Mehrpooya et al., 2018) mainly include direct expansion (Franco and Casarosa, 2015; Gómez et al., 2014), Brayton cycle (Angelino and Invernizzi, 2011; Rovira et al., 2013), Stirling cycle (Renzi and Brandoni, 2014), organic Rankine cycle (Badami et al., 2018; Bao et al., 2017; Sadreddini et al., 2018; Sun et al., 2018; Xue et al., 2017; Zhang et al., 2017, 2018) and so on (García et al., 2016; Ghaebi et al., 2018; Mosaffa et al., 2017; Zhang et al., 2016). Among them, organic Rankine cycle has the characteristic of the high efficiency, simple system structure and mature technology, and can effectively

recover low-grade heat source (Boyaghchi and Sohabatloo, 2018; Mehrpooya et al., 2016; Nemati et al., 2018).

According to the literature review, the two problems of LNG receiving terminal have been studied separately by many scholars, and the overall power consumption of LNG receiving terminal has not been considered. In the BOG management system, cold energy in the LNG regasification process is not considered (E. Querol et al., 2011; Hasan et al., 2009; Park et al., 2010). For cold energy recovery of LNG, the export parameters of LNG storage tanks is selected as the parameters of LNG (Bao et al., 2018; Dispenza et al., 2009; Dong et al., 2013; Lu and Wang, 2009; Oliveti et al., 2012; Parikhani et al., 2019; S. Sadaghiani et al., 2018; Soffiato et al., 2015; Sung and Kim, 2016; Wang and Zhang, 2017). However, the BOG treatment method and generation rate will directly affect the cold energy power generation system of the LNG regasification process. Therefore, it is unreasonable to study these two processes separately, and therefore, this paper proposes the idea of integrating BOG recondensation with LNG cold energy power generation. It uses power generated by cold energy in LNG regasification process to drive the compressor and LNG pump in the BOG recondensation process, so as to reduce the power consumption of the whole LNG receiving terminal and the waste of energy. The main structure of this paper is as follows: Firstly, four BOG recondensation systems are selected in this paper for parameter analysis and power consumption comparison. Then, the cold energy recovery potential of the BOG recondensation system is analyzed, and the cold energy released by the LNG regasification process is recovered by the organic Rankine cycle. Through the parameter analysis and working fluid selection of the integrated system with organic Rankine cycle, the optimal operating conditions of different systems are obtained. Finally, the power consumption of integrated system and non-integrated system at different BOG content are compared.

2. BOG recondensation system

According the previous studies in the references (Nagesh Rao and Karimi, 2018), this paper selects four BOG recondensation systems: one-stage recondensation system, one-stage recondensation system with pre-cooling and after-cooling, one-stage recondensation system with two-stage compression, two-stage recondensation system. The schematic diagrams of four systems are shown in Fig. 1.

One-stage recondensation system is shown in Fig. 1 a) case1. BOG produced in the LNG storage tank is pressurized in the compressor, and enters the recondenser. LNG flows into the recondenser after being pressurized by low-pressure LNG pump. LNG and BOG undergo contact heat exchange in the recondenser, and BOG is completely condensed by subcooled LNG. LNG at the outlet of the recondenser is directly pressurized to the pressure of the pipe network by the LNG high-pressure pump. Finally, the LNG is heated by seawater to a specified temperature and delivered to the user.

One-stage recondensation system with pre-cooling and after-cooling is shown in Fig. 1 b) case 2. On the basis of case 1, case 2 uses one branch of LNG to cool the inlet temperature of the BOG compressor, and the other branch enters the recondenser to condense BOG. Two branches of LNG are mixed at the outlet of the recondenser and then pressurized by the LNG high-pressure pump. The high-pressure LNG is passed through aftercooler for cooling the inlet temperature of the recondenser. Finally, the seawater is used to heat the LNG to a prescribed temperature.

One-stage recondensation system with two-stage compression is shown in Fig. 1 c) case 3. BOG is precooled through precooler, pressurized by the compressor 1, and intercooled with intercooler. Then, BOG enters the compressor 2 for pressurization, and

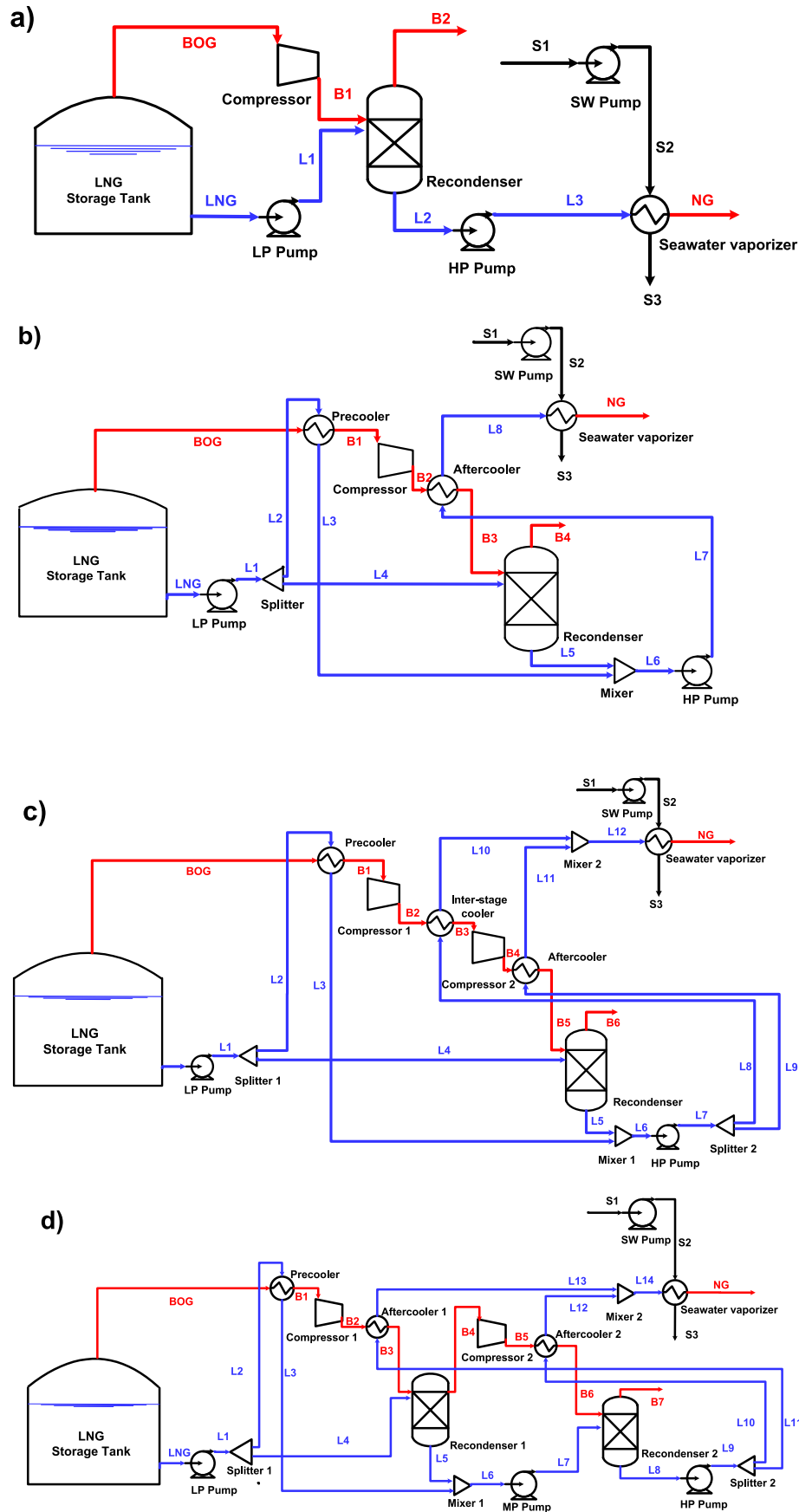


Fig. 1. The schematic diagram of BOG recondenser a) case 1 one-stage recondensation system b) case 2 one-stage recondensation system with pre-cooling and after-cooling c) case 3 one-stage recondensation system with two-stage compression d) case 4 two-stage recondensation system.

aftercools in the aftercooler. Finally enters the recondenser to mix with the LNG and condense. The LNG at the outlet of the recondenser is pressurized by the LNG high pressure pump and divided into two branches, which are used to cool the outlet temperatures of the compressor 1 and compressor 2, respectively. Then the two branches are mixed and heated up to the specified temperature.

Two-stage recondensation is shown in Fig. 1 d) case 4. BOG first enters the precoolers for precooling, and is pressurized by compressor 1. After that, BOG enters the aftercool 1 for aftercooling, and enters the recondenser 1. LNG is pressurized by the LNG low-pressure pump and divided into two branches. One branch of LNG is used to precool the BOG, and the other branch enters the recondenser 1 to partially condense the BOG. The uncondensed BOG enters the compressor 2 to pressurize, then enters the aftercooler 2 to cool with a high-pressure LNG and further enters the recondenser 2. LNG enters the LNG medium-pressure pump from the recondenser 1, and enters the recondenser 2 to completely condense the BOG. The LNG at the outlet of the recondenser 2 is pressurized by the LNG high-pressure pump and divided into two branches, which are used to cool the inlet temperature of the recondenser 1 and recondenser 2, respectively. Then the two branches are mixed and heated up to the specified temperature.

3. Thermodynamic model and parameters

3.1. Thermodynamic model

In order to better perform thermodynamic analysis on the systems, the following assumptions are made during the systems simulation:

1. Each system is in a steady state.
2. In all systems, the pressure change of components except the pump, compressor and turbine are negligible.
3. The change of kinetic energy and potential energy in the system can be neglected, the friction losses in the pipeline and heat exchanger are neglected, and the energy loss of the splitter is negligible.
4. The mechanical energy losses of pumps, compressors and turbines are negligible, and the conversion efficiency between mechanical energy and electrical energy is 100% (Ferreira et al., 2017).

This paper analyzes the power consumptions of the main components of the systems according to the first law of thermodynamics. The main power consuming components in the systems include pumps and compressors. The pump's power consumption mainly comes from sea water pump, LNG pump and working fluid pump. The calculation formulas are as follows:

$$W_{sea,i} = m_{sea,i}(h_{sea,i,out} - h_{sea,i,in})/\eta_{sea,i} \quad (1)$$

$$W_{LNG,i} = m_{LNG,i}(h_{LNG,i,out} - h_{LNG,i,in})/\eta_{LNG,i} \quad (2)$$

$$W_{WF} = m_{WF}(h_{WF,out} - h_{WF,in})/\eta_{WF} \quad (3)$$

The formula for the power required for the compressor is as follows:

$$W_{C,i} = m_{C,i}(h_{C,i,out} - h_{C,i,in})/\eta_{C,i} \quad (4)$$

The main output power component in the LNG receiving terminal is the turbine, and its formula is as follows:

$$W_{tur} = \eta_{tur} m_{tur}(h_{tur,in} - h_{tur,out}) \quad (5)$$

The power consumption of the overall LNG receiving station is:

$$W_{PC} = \sum W_{sea,i} + \sum W_{LNG,i} + W_{WF} + \sum W_{C,i} - W_{tur} \quad (6)$$

In the above formulas, m represents the mass flow of the stream, h represents the specific enthalpy of the state point, η represents the efficiency of the component, and i represents the number of pumps or compressors. C means the compressor, and tur means the turbine. PC is the power consumption of system.

3.2. System parameter

In this paper, the systems are simulated by Aspen Hysys software. The thermodynamic parameters required by the system in the simulation process are listed in Table 1. The Peng-Robinson equation is used to calculate the thermodynamic properties (Lee, 2017). The composition of BOG and LNG selected in this paper are shown in Table 2 (Noh et al., 2018). This paper realizes the connection between Aspen hysys software and Matlab software through Active X control, and optimizes the parameters of the system by using the genetic algorithm in Matlab toolbox. In the simulation process, in order to ensure the normal progress of the heat exchange and effective heat exchange area, the pinch point of the heat exchanger is required to be larger than 5 °C. In order to achieve zero emission of BOG, the mass flow rate at the outlet of the recondenser is required to be zero. In order to ensure production safety, the condenser cannot have negative pressure, so the condensing pressure should be higher than 100 kPa.

3.3. Working fluid selection

The working fluid has an important impact on the performance of LNG cold energy power generation system. The suitable working fluid can effectively increase the power generation capacity of the LNG cold energy power generation system. However, due to the particularity of the application, the chemical and thermodynamic properties of the working fluid are required to be stable (Li et al., 2016). In the process of selecting the working fluid, in order to ensure the safety of production, the condenser cannot produce negative pressure, so the condensation temperature in the system is higher than the normal boiling point of the working fluid. The LNG regasification process is from storage temperature (−162 °C) to near ambient temperature (10 °C), which requires working fluids with the low normal boiling points. At the same time, the working fluid is also prevented from being frozen during the cycle. Therefore, the number of working fluids those meet the requirements are

Table 1
The thermodynamic parameter of system.

Parameter	Value
The temperature of BOG (°C)	−120
The pressure of BOG (kPa)	100
The temperature of LNG (°C)	−162
The pressure of LNG (kPa)	100
The temperature of seawater (°C)	15
The pressure of seawater (kPa)	100
Isentropic efficiency of compressor (%)	70
Isentropic efficiency of pump (%)	80
Isentropic efficiency of turbine (%)	80
Minimum approach temperature in heat exchanger (°C)	5
Discharge pressure of seawater pump (kPa)	300
Mass flow of NG (kg/h)	36000
Regasification pressure of LNG (kPa)	7000

Table 2
The composition of BOG and LNG.

Composition (mole fraction)	BOG	LNG
CH ₄	0.8788	0.9133
C ₂ H ₆	0.0001	0.0536
C ₃ H ₈	—	0.0214
i-C ₄ H ₁₀	—	0.0047
n-C ₄ H ₁₀	—	0.0046
i-C ₅ H ₁₂	—	0.0001
n-C ₅ H ₁₂	—	0.0001
N ₂	0.1211	0.0022

small, and are mainly HCs and HFCs (Gómez et al., 2014; He et al., 2015; Lee and Kim, 2015; Lee et al., 2014; Rao et al., 2013; Sung and Kim, 2016; Zhang et al., 2016). It is considered that the working fluid may have an impact on the environment, and the GWP of the fourth generation refrigerant is ≤ 150 stipulated in the *Kyoto Protocol* (Calm JM, 2011). In this paper, six working fluids are selected considering the above factors. The thermodynamic properties of the working fluid are listed in Table 3.

4. Results and discussion

4.1. Influence of parameters on power consumption of BOG recondensation systems

Firstly, this section analyzes the effects of the key parameters of the BOG recondensation system. Because the influence of the parameters of the other three BOG recondensation systems on the system performance is similar to that of case 4, considering the length of the article, this paper selects the most complex recondensation system case 4 as an example for parameter analysis. The effect of system parameters on the power consumption of case 4 are shown in Fig. 2.

Firstly, the impact of outlet pressure of compressor 1 is analyzed. It can be seen from Fig. 2 a) that there is an optimum value for the outlet pressure P_{B2} of compressor 1 to minimize the power consumption of the system. As the P_{B2} increases, the amount of BOG that can be condensed in the recondenser 1 increases, and the amount of BOG at the outlet of the recondenser 1 decreases. When the outlet pressure of compressor 2 is constant, the mass flow rate of vapor at the inlet of compressor 2 is reduced and the power consumption of the compressor 2 is reduced. The reduction of the power consumption of compressor 2 is larger than the increase of power consumption of compressor 1, so power consumption of the whole system is reduced. However, as P_{B2} continues to increase, the mass flow rate of vapor at the outlet of recondenser 1 gradually decreases, and the situation is reversed. Therefore, when the pressure P_{B2} reaches a certain value, the power consumption of the system will increase as P_{B2} increases. Therefore, there is an optimal value for P_{B2} that minimizes power consumption.

Fig. 2 b) depicts the effect of the outlet pressure P_{B5} of compressor 2 on power consumption. Because the zero emission of

BOG is required, the flow rate of vapor at the outlet of the recondenser 2 is 0. Therefore, the influence of this limitation on the parameters is considered in the analysis process. It can be seen from Fig. 2 b) that as P_{B5} increases, the power consumption of the system gradually increases, and the mass flow of vapor at the outlet of the recondenser 2 gradually decreases. When the outlet pressure of the compressor 2 reaches a certain value, the amount of BOG at the outlet of the recondenser is zero. Because the pressure at the outlet of the LNG pump is also increasing as the outlet pressure of the compressor rises, the pressurized LNG carries more cold energy and can condense more BOG. However, the greater the outlet pressure of the compressor is, the higher the power consumption of the system will be. The confinement that the mass flow rate of vapor at the outlet of the recondenser is zero should be satisfied, so the outlet pressure of the compressor 2 has an optimum value, which minimizes the power consumption of the system.

The relationship between the flow ratio of low-pressure LNG L2 for precooling and the power consumption is shown in Fig. 2 c). As the flow ratio L2 increases, the power consumption of the system decreases firstly and then increases. The heat transfer amount in the precooling gradually increases as the flow ratio of L2 increases, and the inlet temperature of the compressor gradually decreases, so the power consumption of the compressor gradually decreases. However, as the flow ratio of L2 continues to increase, the amount of LNG entering the recondenser is insufficient to completely condense the BOG. Therefore, more BOG enters the compressor 2 to be pressurized, and eventually the system's power consumption is gradually increased.

Fig. 2 d) and 2 e) show the effects of inlet temperatures of two recondenser on power consumption. It can be seen from Fig. 2 d) that as the inlet temperature of the recondenser 1 increases, the power consumption of the system gradually increases. The BOG outlet temperature of the recondenser 1 rises as the inlet temperature of the recondenser 1 increases, resulting in the rise of the inlet temperature of the compressor 2 rises, so the power consumption of the compressor rises. It can be seen from Fig. 2 e) that the inlet temperature of the recondenser 2 has little effect on the power consumption of the system under the condition that other parameters are fixed. However, the lower inlet temperature of recondenser 2 will cause the required condensing pressure in the recondenser 2 to decrease, which will affect the outlet pressure of compressor 2, so it needs to be optimized.

4.2. Comparison of power consumptions for BOG recondensation systems

Section 4.1 analyzes the key parameters of case 4. From the results, it can be seen that the parameters have significance influence and should be optimized. In this section, the parameters of the four BOG recondensation systems are optimized and the power consumptions are compared under the condition of BOG content of 0.15. The parameters and optimization range are shown in Table 4. The comparisons of the power consumptions are shown in Fig. 3. The results of parameter optimization of the system are listed in

Table 3
The thermodynamic properties of working fluids (Zhang et al., 2017).

Working fluid	Chemical formula	Normal boiling temperature (°C)	ODP	GWP	Safety
R150	C ₂ H ₄	-103.7	0	120	A3
R170	C ₂ H ₆	-88.6	0	-20	A3
R41	CH ₃ F	-78.55	0	-20	A1
R1270	C ₃ H ₆	-47.7	0	-20	A3
R290	C ₃ H ₈	-42.17	0	20	A3
R152a	C ₂ H ₄ F ₂	-25	0	120	A2

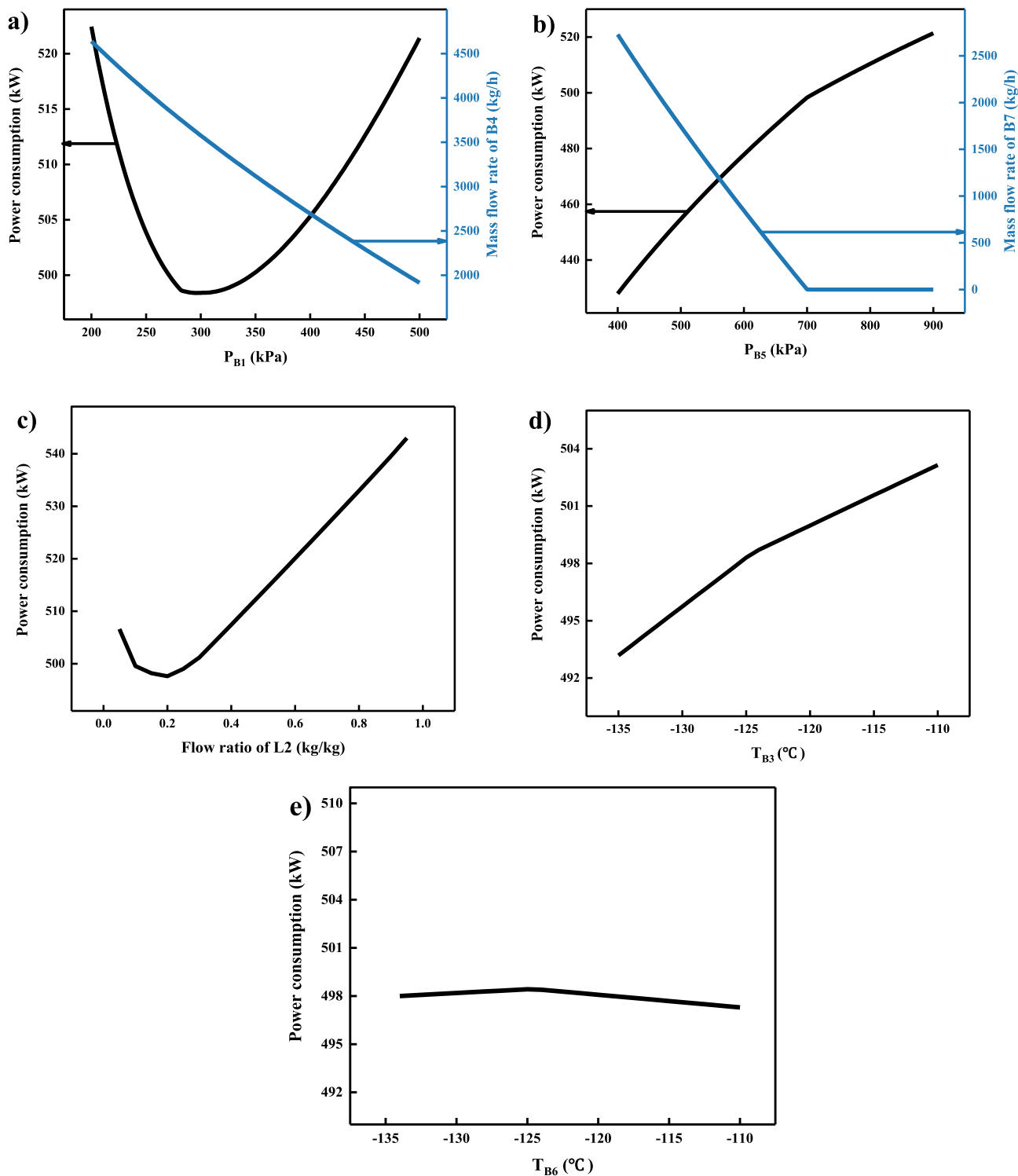


Fig. 2. Influence of parameters on power consumption for case 4 a) outlet pressure of compressor 1 b) outlet pressure of compressor 2 c) the flow ratio of L2 d) inlet temperature of recondenser 1 e) inlet temperature of recondenser 2.

Table 5.

As seen from Fig. 3, case 4 has a power consumption of 491.7 kW, which is the lowest, followed by case 3, case 2, and case 1. It can be also seen from the power consumption ratio of each component that the compressor is the main power consuming component in the BOG recondensation systems. Therefore, reducing the power consumption of the compressor can effectively reduce the power

consumption of the system. In order to better explain the difference of power consumption caused by different systems, the p-h diagrams of case 2, case 3 and case 4 are compared with case 1 in Fig. 4.

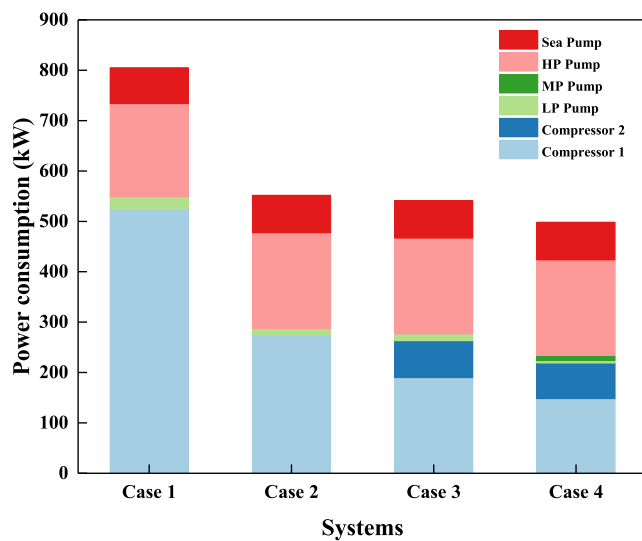
Compared to case 1, the power consumption of case 2 is reduced by 31% in Fig. 3.

It can be seen from Fig. 4 a) that the system case 2 reduces the power consumption of the compressor by reducing the inlet

Table 4

The parameters and optimization range.

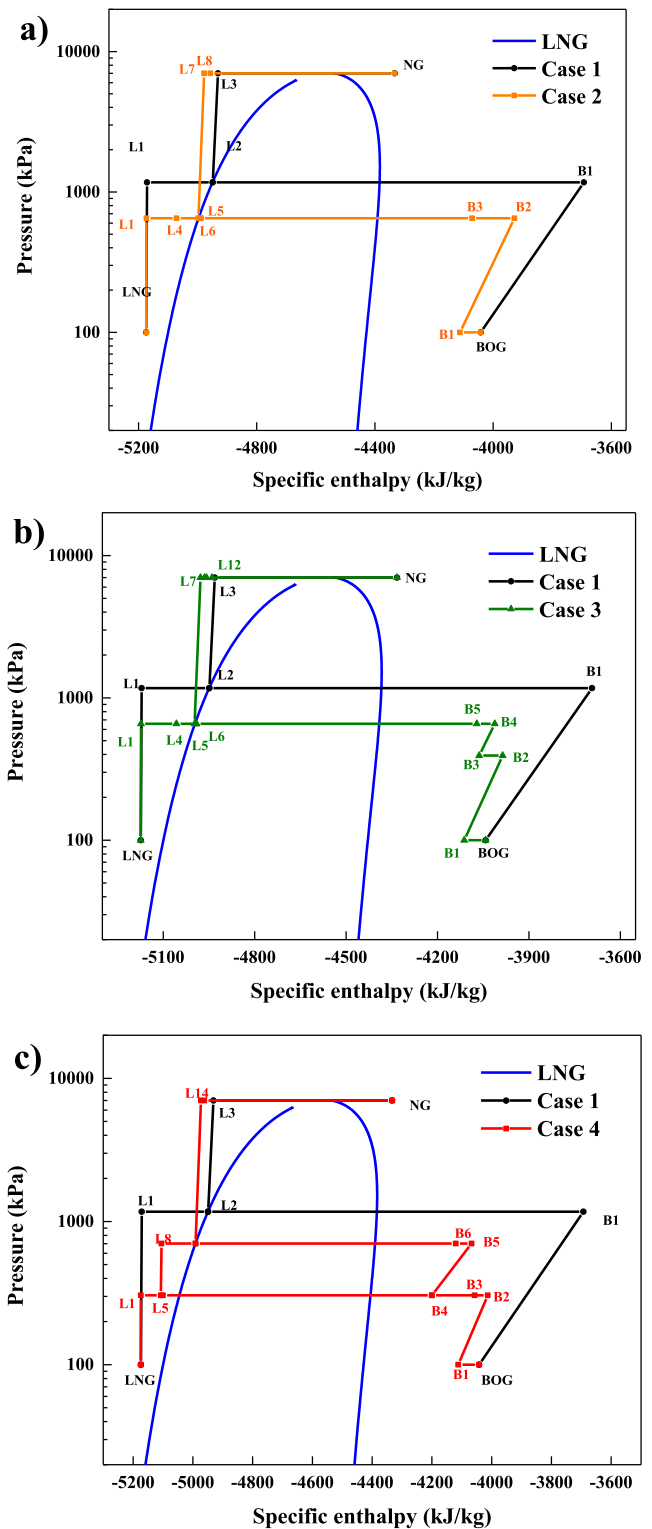
Systems	Parameters	Optimization range
Case 1	P_{B1} (kPa)	[100,1500]
Case 2	P_{B2} (kPa)	[100,1000]
	Flow ratio of L2	[0,1]
	T_{B3} ($^{\circ}\text{C}$)	[-140, -110]
Case 3	P_{B2} (kPa)	[100,500]
	P_{B4} (kPa)	[400,1000]
	T_{B5} ($^{\circ}\text{C}$)	[-140, -110]
	Flow ratio of L2	[0,1]
	Flow ratio of L8	[0,1]
Case 4	P_{B2} (kPa)	[100,500]
	P_{B5} (kPa)	[400,1000]
	T_{B3} ($^{\circ}\text{C}$)	[-140, -110]
	T_{B6} ($^{\circ}\text{C}$)	[-140, -110]
	Flow ratio of L2	[0,1]
	Flow ratio of L10	[0,1]

**Fig. 3.** Comparison of power consumptions of BOG recondensation systems.**Table 5**

The optimization results of the systems.

System	Parameter	Value
Case1	P_{B1} (kPa)	1170.20
	W_{PC} (kW)	805.05
Case2	P_{B2} (kPa)	649.46
	Flow ratio of L2	0.11
	T_{B2} ($^{\circ}\text{C}$)	-126.67
	W_{PC} (kW)	551.87
Case3	P_{B2} (kPa)	397.88
	P_{B4} (kPa)	649.42
	T_{B5} ($^{\circ}\text{C}$)	-126.69
	Flow ratio of L2	0.12
	Flow Ratio (L7)	0.54
	W_{PC} (kW)	540
	P_{B2} (kPa)	305.33
	P_{B5} (kPa)	700.90
Case4	T_{B3} ($^{\circ}\text{C}$)	-124.76
	T_{B6} ($^{\circ}\text{C}$)	-124.98
	Flow ratio of L2	0.24
	Flow ratio of L9	0.70
	W_{PC} (kW)	497.10

temperature of the compressor. At the same time, case 2 uses high-pressure LNG to reduce the inlet temperature of the recondenser,

**Fig. 4.** The p-h diagrams of BOG recondensation systems a) case 1 and case 2, b) case 1 and case 3, c) case 1 and case 4.

resulting in the decrease of the condensing pressure in the recondenser and the pressure required by the compressor. Ultimately, the purpose of reducing compressor power consumption is achieved.

The power consumption of case 3 is reduced by 33% compared

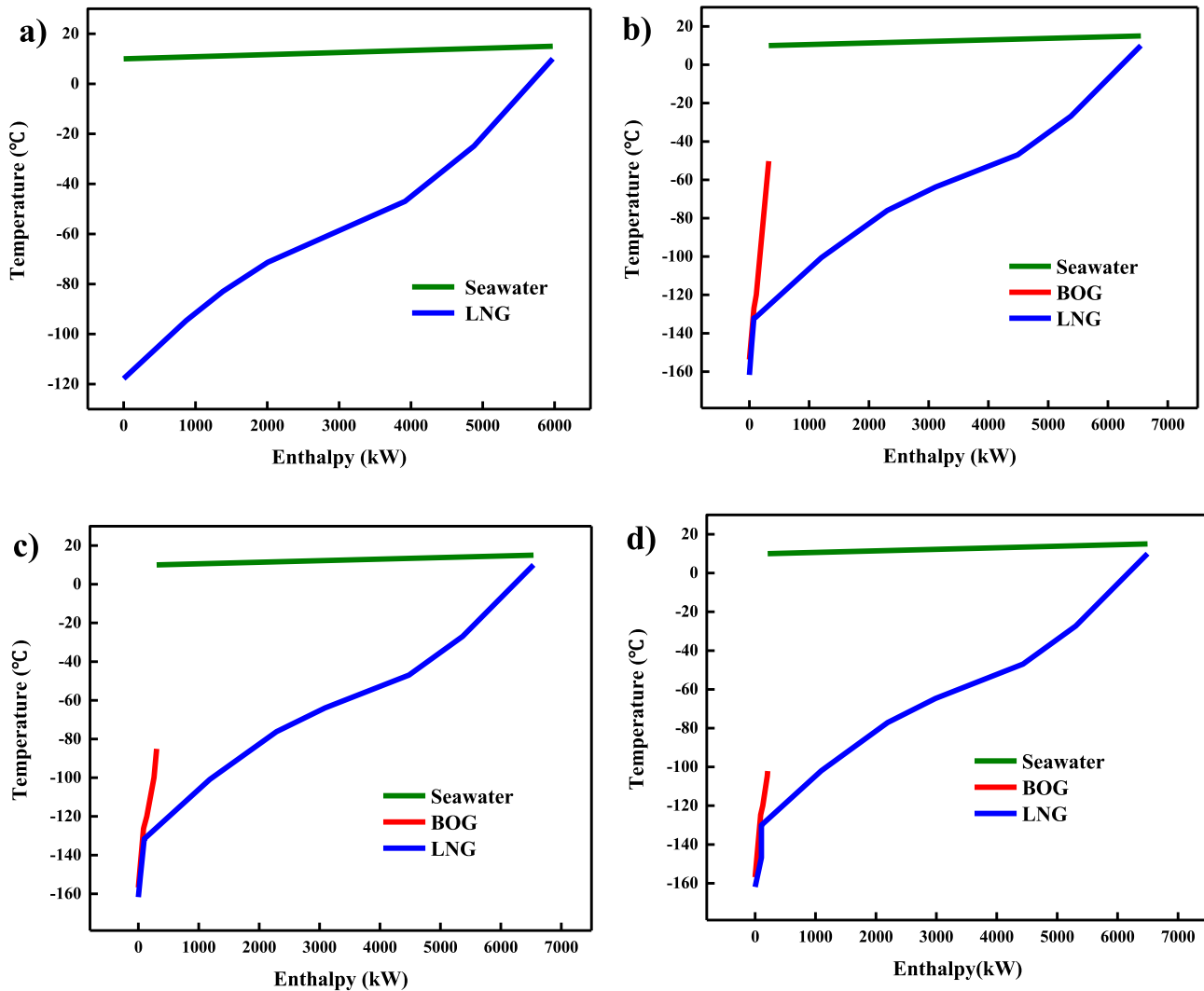


Fig. 5. The T-H diagrams of BOG reconcondensation systems a) case 1, b) case 2, c) case 3 and d) case 4.

with case 1 in Fig. 3. For one-stage reconcondensation system with one-stage compression, when the BOG content is high, the pressure ratio of the compressor is too high. If the compressor's pressure ratio is too high, the volumetric efficiency of the compressor will decrease, the power consumption will increase and the exhaust temperature will be high.

One-stage reconcondensation system with two-stage compression, using high-pressure LNG to reduce the temperature of BOG entering the compressor 2, can effectively avoid the above problems, and can effectively reduce the power consumption of the compressor.

In Fig. 3, the power consumption of case 4 is 38% lower than that of case 1. It can be seen from Fig. 4 c) that the recondenser 1 in case 4 only partially condenses BOG, and does not require excessively high condensing pressure. The outlet pressure of the compressor 1 is reduced, so the power consumption of the compressor 1 is decreased. Since a part of the BOG condenses in the recondenser 1, the amount of BOG entering the compressor 2 is reduced, so the power consumption of the compressor 2 is reduced. At the same time, the temperature of the BOG entering the compressor 2 can be lowered by the recondenser 1, and finally the purpose of reducing the power consumption of the BOG reconcondensation system is achieved.

4.3. Utilization of cold energy in LNG regasification process

According to the analysis of power consumptions for the BOG reconcondensation systems in section 4.2, although the structural improvement can reduce the power consumption of the system, the BOG reconcondensation process is still a high power-consuming process. In order to further reduce the power consumption of the BOG reconcondensation process, this section analyzes the heat transfer process of the system and tries to find the potential of the cold energy recovery. The T-H diagrams of the four BOG reconcondensation systems are shown in Fig. 5. The T-H diagram is mainly used to describe the heat transfer matching problem between cold and hot streams in the process system (Fernández-Polanco and Tatsumi, 2016; Kemp, 2007; Le et al., 2018; Manizadeh et al., 2018; Smith, 2005; Souifi and Souissi, 2019).

It can be clearly seen from Fig. 5 that the cold energy released during the LNG regasification process is carried away by the seawater, resulting in extreme waste of energy. If the cold energy can be recovered, the energy waste can be effectively reduced. This section proposes four integrated systems of BOG reconcondensation process and LNG cold energy power generation system. The cold energy of the LNG regasification process is recovered by the organic Rankine cycle for power generation. The schematic diagrams of

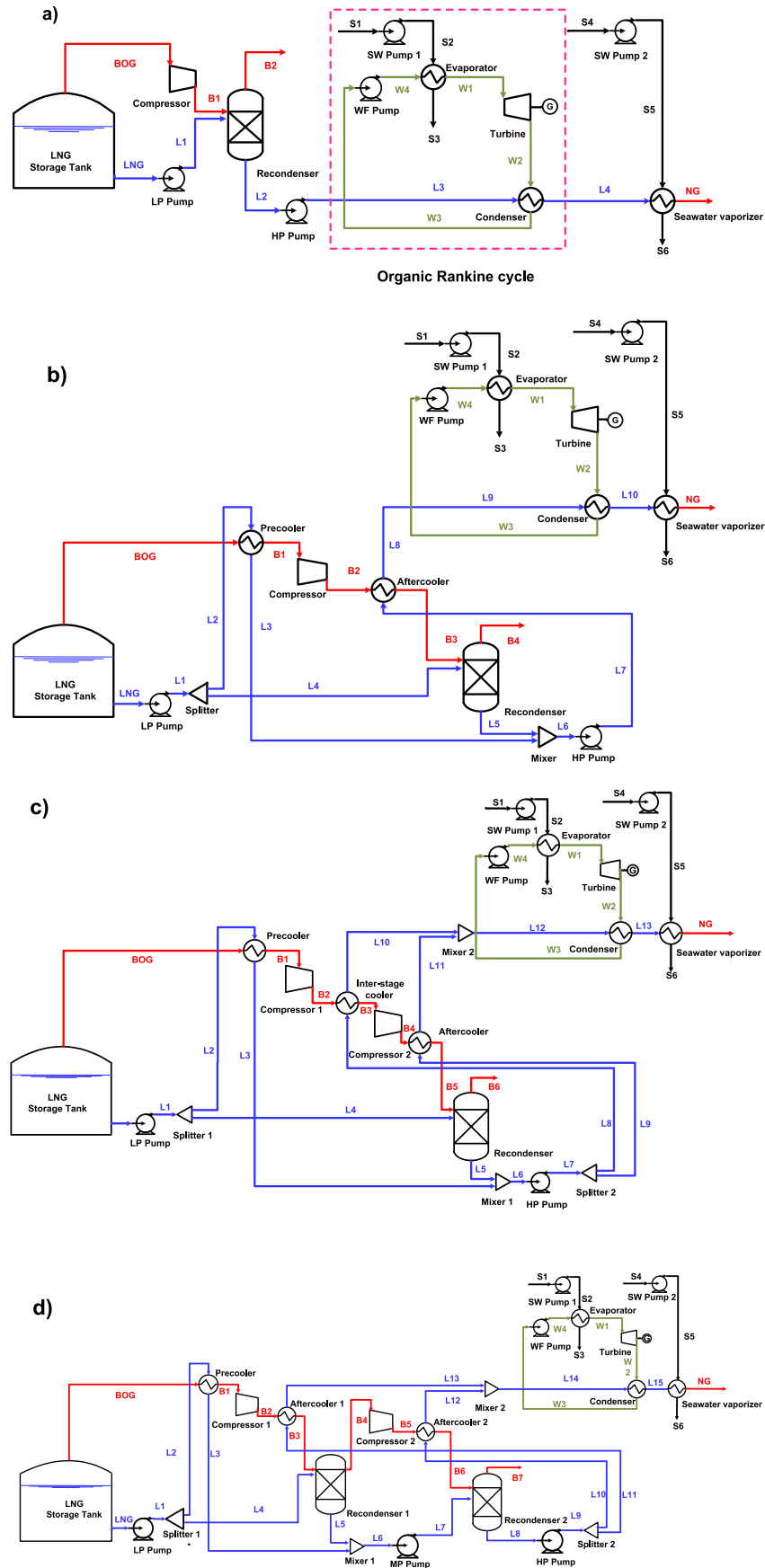


Fig. 6. Four integrated systems of BOG recondensation process and LNG cold energy power generation system a) case 5, b) case 6, c) case 7 and d) case 8.

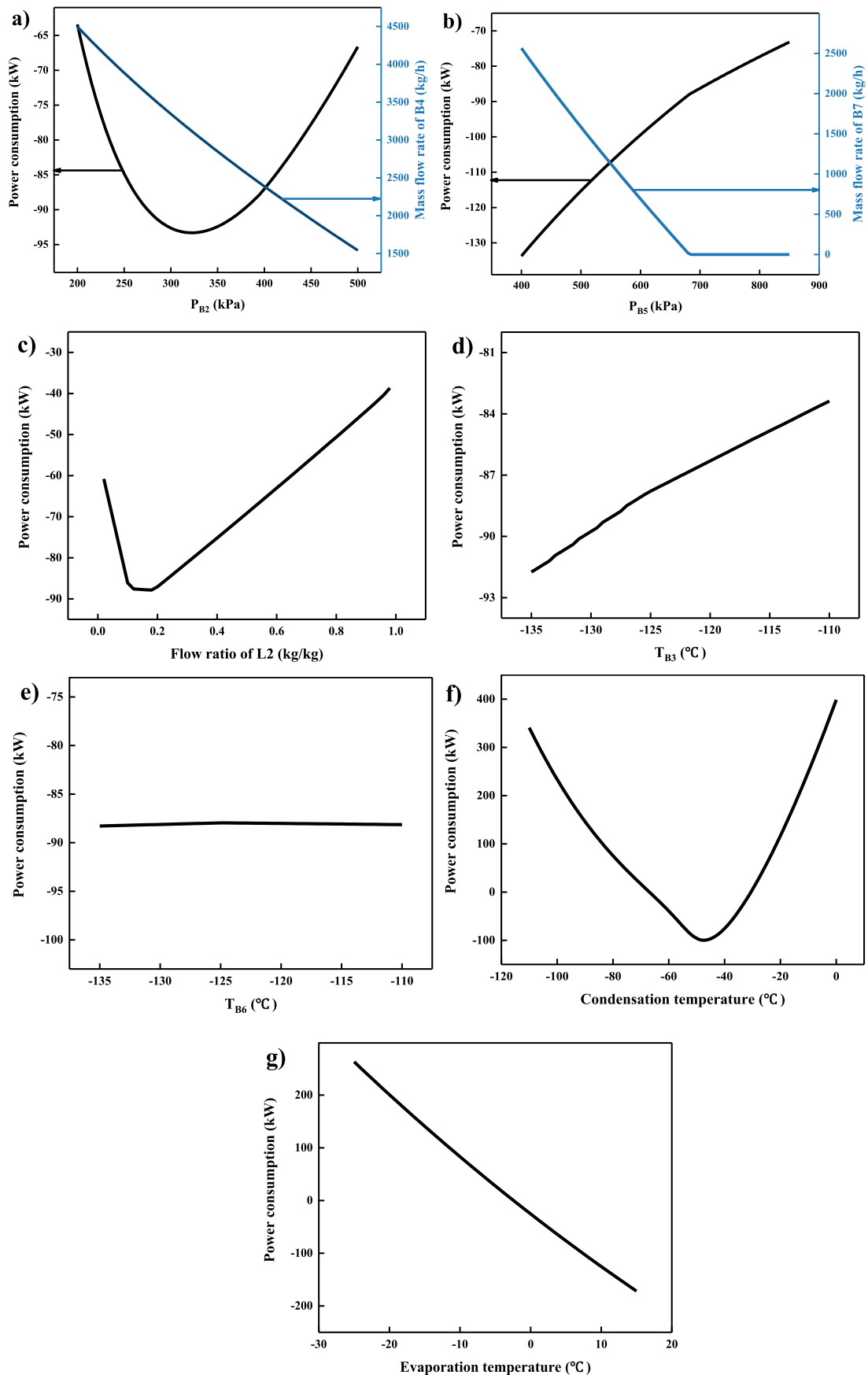


Fig. 7. Influences of parameters on power consumptions of BOG recondensation systems a) outlet pressure of compressor 1, b) outlet pressure of compressor 2, c) flow ratio of L2, d) inlet temperature of recondenser 1, e) inlet temperature of recondenser 2, f) condensation temperature and g) evaporation temperature.

integrated systems are shown in Fig. 6. The structure of the organic Rankine cycle is shown in the dotted line in Fig. 6 a). The working fluid is heated by seawater in the evaporator to become saturated vapor of high pressure, and then enters the turbine to generate electricity by expansion. Then the working fluid enters the condenser to recover the cold energy released by the LNG vaporization process, and becomes a low temperature and low-pressure saturated liquid. Finally, the working fluid is pressurized by the working fluid pump and then enters the evaporator for the next cycle. LNG enters the condenser from the LNG high-pressure pump and exchanges heat with the working fluid. At last, LNG is heated by seawater to the specified temperature.

4.4. Effects of operating conditions on power consumption of integrated systems

4.4.1. The effect of key parameters on power consumption

In order to reduce the power consumption of the BOG recondensation systems, four integrated systems of BOG recondensation process and LNG cold energy power generation are proposed in section 4.3, which use the organic Rankine cycle to recover the cold energy generated by the LNG regasification process to drive the BOG recondensation process. For the integrated system case 5, case 6 and case 7, the evaporation temperature and condensing temperature of the Rankine cycle have similar effects on the system power consumption as the system case 8. In this section, case 8 is taken as an example to analyze the influence of the key parameters with the BOG content of 0.15 and R290 as working fluid. The effect of system parameters on power consumption are shown in Fig. 7. It should be pointed out that the negative power consumption in this section is the result of a larger output work of turbine in ORC system than the power consumption in BOG recondensation process, and the system has the ability to output work.

The parameters of the BOG recondensation process have the same rule as those of the system in section 4.1, and will not be explained further here. Fig. 7 f) shows the effect of the condensation temperature of the organic Rankine cycle on the power consumption of the system. It can be seen that there is an optimal condensation temperature to minimize the power consumption of the system. Because the evaporation temperature and the flow rate of LNG are constant, as the condensation temperature increases, the LNG cold energy that the system can recover increases, and the system can process more work. However, as the condensing temperature increases further, the outlet pressure of the turbine increases, resulting in a decrease of output work of turbine. The two combined effect results in an optimal condensation temperature in the system that minimizes power consumption.

Fig. 7 g) displays effect of the evaporation temperature of the organic Rankine cycle on system power consumption. As the evaporation temperature increases, the power consumption of the system gradually decreases. When the condensation temperature is constant, according to the Carnot's theorem, the maximum efficiency of the ORC system increases with the increase of the evaporation temperature. Therefore, the system's power consumption is reduced.

4.4.2. The effect of working fluids

In section 4.3.1, the key parameters of the system are analyzed with BOG content of 0.15 and R290 as working fluid. The suitable working fluid can effectively improve the performance of the organic Rankine cycle system. Therefore, six working fluids are selected in this section to investigate the effect of working fluid on system power consumption under the best working conditions. In addition to optimizing the key parameters in Table 4, this section also needs to optimize the condensation temperature and

evaporation temperature of the system. The optimization ranges of the condensation temperature and evaporation temperature are $[-110^{\circ}\text{C}, 0^{\circ}\text{C}]$ and $[-10^{\circ}\text{C}, 10^{\circ}\text{C}]$, respectively. The system power consumptions of different working fluids are shown in Fig. 8. The optimization results of system parameters are listed in Table 6.

It can be seen from Fig. 8 that the order of the integrated system's power consumption is not affected by the working fluids. Case 8 has the lowest power consumption, followed by case 7, case 6, and case 5. The power consumption of the four integrated systems are ranked in the same order as the corresponding four BOG recondensation systems.

From Fig. 8, R1270 has the lowest power consumption. The effects of the condensation temperatures of different working fluids on the system power consumption are shown in Fig. 9. At the optimum condensation temperature, the system has the lowest power consumption when the working fluid is R152a. However, the normal boiling point of R152a is higher than the optimal condensation temperature. Because the condensation pressure needs to be limited during the simulation optimization process, the optimized power consumption is higher than the power consumption at the optimal condensation temperature. The normal boiling point of R1270 is near its optimum condensation temperature, so the system has the lowest power consumption when the working fluid is R1270.

4.4.3. The effect of BOG content on power consumption

The difference of BOG content will directly affect the power consumption of the BOG recondensation system and the power generation of the LNG cold power generating system. Therefore, when R1270 is used as the working fluid at different BOG contents, power consumption between integrated systems and non-integrated systems are compared. The change trend of power consumption of each system at different BOG content is shown in Fig. 10. The optimization results of variables are shown in Table 7 and Table 8.

It can be seen from Fig. 10 a) that the power consumption of the system gradually decreases as the BOG content increases. On the one hand, as the BOG content increases, the outlet pressure of the compressor in the system increases, resulting in an increase of compressor power consumption. On the other hand, as the capacity of BOG treatment increases, more LNG cold energy is consumed in the recondenser for condensing BOG, resulting in a decrease in LNG

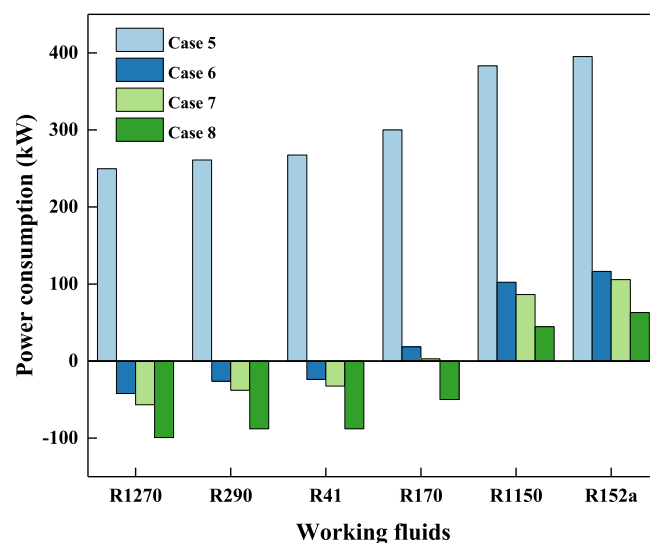


Fig. 8. Influences of working fluids on power consumption in integrated system.

Table 6
Optimization results of integrated system with different working fluids.

Systems	Parameters	Working fluids					
		R1150	R170	R290	R1270	R41	R152a
Case 5	P_{B1} (kPa)	1170.3	1170.3	1170.3	1170.3	1170.3	1175.0
	T_{W1} (°C)	-47.47	-46.58	-42.45	-42.73	-46.45	-24.60
	T_{W3} (°C)	5.62	6.92	6.18	6.19	6.51	5.65
	W_{PC} (kW)	383.11	300	260.93	249.68	267.47	395.23
	P_{B2} (kPa)	645.46	639.46	651.93	653.18	650.07	649.53
	Flow Ratio of L2	0.0974	0.0894	0.1290	0.1311	0.1138	0.1195
	T_{B3} (°C)	-126.82	-126.86	-126.52	-126.64	-126.50	-126.64
Case 6	T_{W1} (°C)	-47.93	-47.07	-42.30	-47.70	-47.35	-24.72
	T_{W3} (°C)	5.67	6.95	6.13	6.21	6.49	5.69
	W_{PC} (kW)	102.24	18.49	-26.09	-42.07	-23.7	116.46
Case 7	P_{B2} (kPa)	388.96	404.16	428.68	398.74	412.51	389.97
	P_{B4} (kPa)	650.14	669.88	658.18	650.18	669.90	652.56
	T_{B5} (°C)	-126.48	-126.73	-126.70	-126.48	-126.73	-126.45
	Flow ratio of L2	0.1108	0.1516	0.1374	0.1216	0.1516	0.1297
	Flow ratio of L8	0.5211	0.2711	0.5262	0.5025	0.6427	0.2525
	T_{W1} (°C)	-48.56	-47.31	-42.25	-47.43	-47.39	-24.77
	T_{W3} (°C)	5.54	6.95	6.14	6.20	6.53	5.54
	W_{PC} (kW)	86.3	2.8	-37.77	-56.65	-32.43	105.75
Case 8	P_{B2} (kPa)	394.52	394.20	394.02	394.01	335.28	373.45
	P_{B5} (kPa)	734.56	681.46	682.46	733.06	692.71	698.69
	T_{B3} (°C)	-125.64	-125.63	-125.54	-125.38	-125.26	-125.48
	T_{B6} (°C)	-125.35	-125.60	-125.35	-125.34	-125.22	-125.10
	Flow ratio of L2	0.1861	0.1861	0.1861	0.1861	0.2289	0.2519
	Flow ratio of L10	0.6067	0.5615	0.5850	0.6468	0.6468	0.5207
	T_{W1} (°C)	-48.31	-47.73	-42.38	-47.54	-47.40	-24.69
	T_{W3} (°C)	5.53	6.98	6.16	6.15	6.53	5.63
	W_{PC} (kW)	44.67	-49.85	-87.97	-99.24	-87.88	62.93

cool energy for power generation and a gradual decrease in power generation of the LNG cold energy system. Therefore, as the BOG content increases, the power consumption of the system gradually increases.

It can be clearly seen from Fig. 10 a) that the power consumption of the four integrated systems are significantly lower than those of four non-integrated systems. It can be seen that the integration of the BOG recondensation process and the LNG cold energy power generation system can effectively reduce the power consumption of the BOG recondensation process. The power reduction rate of the four integrated systems at different BOG content are shown in Fig. 10 b). As the BOG content increases, the power consumption

reduction rate of the integrated system gradually decreases. With the increase of BOG treatment capacity, the power consumption of the BOG recondensation system is gradually increased, and the power generation of the LNG cold energy power generation is gradually reduced, resulting in a gradual decline in the power consumption reduction rate of the integrated system. When the BOG content is 0.15, case 5 has a 69% reduction in power consumption compared to case 1. The power generation of the other three integrated systems not only meets the needs of the BOG recondensation process, but also has excess power output. When the BOG content is less than 0.12, all systems can not only achieve self-sufficiency, but also can output external power, which can be used for other aspects of the LNG receiving terminal. When the BOG content is 0.03, the power consumption reduction rate of the system case 8 reaches 250%.

5. Conclusion

In order to reduce the power consumption of BOG recondensation process, this paper proposes four integrated systems of BOG recondensation process and LNG cold energy generation system. Through the parameter analysis and comparison of power consumptions of the systems, the following conclusions are drawn:

1. The key parameters of the system have an important impact on power consumption. For case 8, the outlet pressure of compressor 1, the low-pressure LNG flow ratio and the condensing temperature of organic Rankine cycle have optimal values to minimize system power consumption. The outlet pressure of the compressor 2 and the inlet temperature of the recondenser 1 are positively correlated with the power consumption of the system, while the evaporation temperature of organic Rankine cycle is negatively correlated with the power consumption of the system.

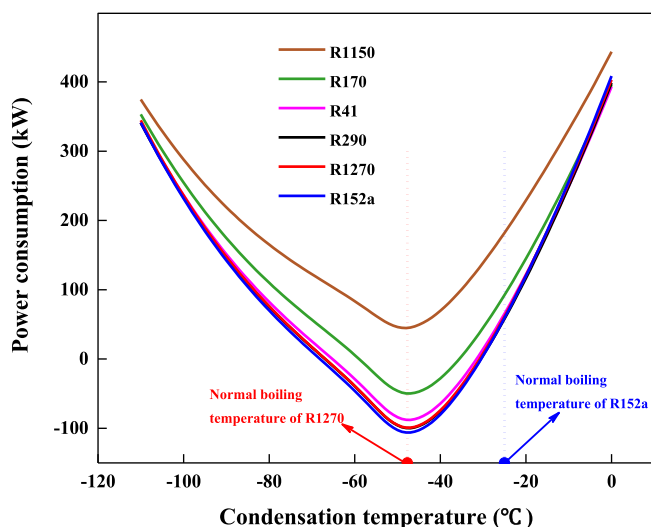


Fig. 9. Influences of condensation temperatures of different working fluids on power consumption.

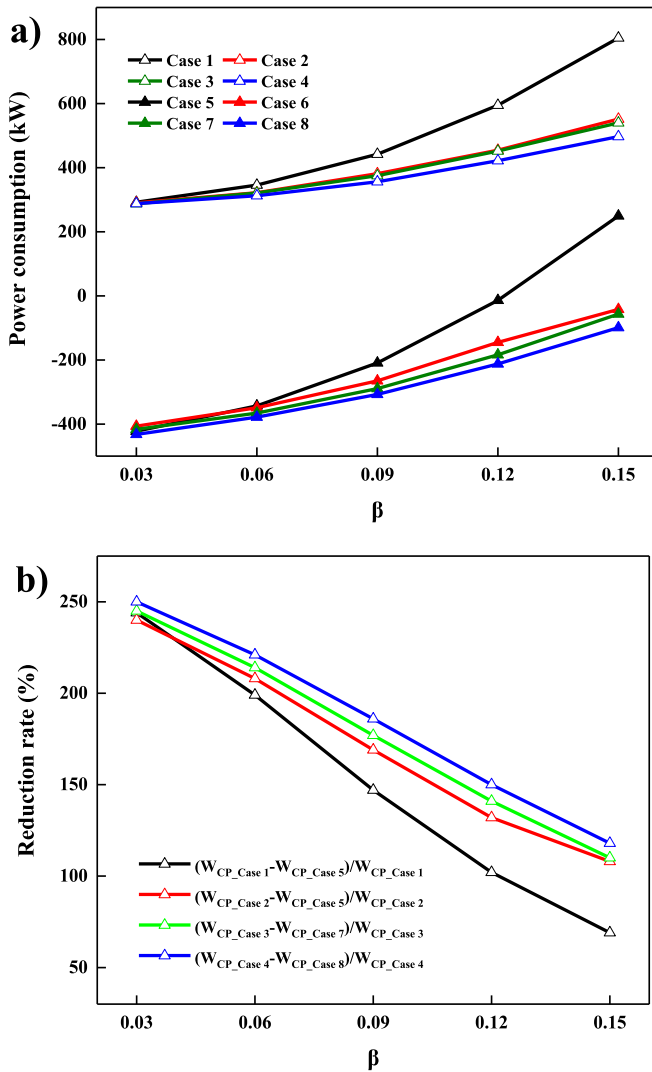


Fig. 10. The influence of BOG content β on a) power consumptions b) power reduction rates of integrated systems.

Table 7
Optimization results of reconcondensation systems at different BOG contents.

Systems	Parameters	β			
		0.03	0.06	0.09	0.12
case 1	P _{B1} (kPa)	159.93	263.66	435.37	718.01
	W _{PC} (kW)	292.38	345.82	442.03	595.12
	P _{B2} (kPa)	173.71	238.03	358.11	481.07
case 2	Flow Ratio of L2	0.02	0.04	0.06	0.08
	T _{B3} (°C)	-148.08	-142.63	-137.61	-131.96
	W _{PC} (kW)	290.46	322.01	381.37	454.83
case 3	P _{B2} (kPa)	140.22	191.48	249.29	330.33
	P _{B4} (kPa)	155.95	237.30	344.34	494.64
	T _{B5} (°C)	-148.39	-142.89	-137.60	-131.97
	Flow Ratio of L2	0.02	0.04	0.06	0.08
	Flow Ratio of L8	0.57	0.32	0.26	0.38
	W _{PC} (kW)	287.65	321.12	375.14	451.84
case 4	P _{B2} (kPa)	157.93	158.92	211.10	270.96
	P _{B5} (kPa)	540.88	242.11	355.05	541.58
	T _{B3} (°C)	-148.37	-142.63	-137.03	-130.68
	T _{B6} (°C)	-147.70	-142.65	-137.05	-127.64
	Flow Ratio of L2	0.02	0.24	0.21	0.21
	Flow Ratio of L10	0.78	0.69	0.82	0.63
	W _{PC} (kW)	288.0	312.45	356.07	421.90

Table 8
Optimization results of integrated system at different BOG contents.

Systems	Parameters	β			
		0.03	0.06	0.09	0.12
case 5	P _{B1} (kPa)	169.55	263.66	435.31	718.00
	T _{W1} (°C)	-47.48	-47.48	-47.48	-47.18
	T _{W3} (°C)	6.14	6.16	6.19	6.21
	W _{PC} (kW)	-422.24	-343.01	-209.41	-14.12
case 6	P _{B2} (kPa)	160.29	237.52	344.28	517.12
	Flow Ratio of L2	0.10	0.07	0.08	0.10
	T _{B3} (°C)	-148.09	-142.85	-137.43	-131.85
	T _{W1} (°C)	-47.60	-47.68	-48.15	-47.70
	T _{W3} (°C)	6.48	6.54	6.55	6.54
	W _{PC} (kW)	-406.36	-349.09	-264.99	-145.14
case 7	P _{B2} (kPa)	184.40	202.38	251.25	316.38
	P _{B4} (kPa)	253.75	264.00	344.34	480.92
	T _{B5} (°C)	-148.43	-142.94	-137.49	-132.06
	Flow Ratio of L2	0.03	0.04	0.06	0.12
	Flow Ratio of L8	0.26	0.21	0.51	0.56
	T _{W1} (°C)	-47.68	-47.68	-47.66	-47.70
	T _{W3} (°C)	6.20	6.20	6.18	6.21
	W _{PC} (kW)	-416.50	-365.60	-289.10	-183.80
	P _{B2} (kPa)	135.76	179.22	216.30	300.11
	P _{B5} (kPa)	172.59	267.32	384.11	549.66
	T _{B3} (°C)	-148.25	-142.62	-137.05	-131.24
case 8	T _{B6} (°C)	-148.27	-142.71	-136.99	-131.00
	Flow Ratio of L2	0.08	0.10	0.14	0.19
	Flow Ratio of L10	0.69	0.40	0.45	0.46
	T _{W1} (°C)	-47.62	-47.61	-47.68	-47.55
	T _{W3} (°C)	6.21	6.09	6.20	6.15
	W _{PC} (kW)	-432.39	-378.50	-307.58	-212.52

- When the BOG content is 0.15, the two-stage reconcondensation system consumes the least power, and the power consumption is reduced by 38% compared with one-stage reconcondensation system.
- With different working fluids, the power consumption of four integrated systems are ranked the same as those of the corresponding BOG reconcondensation systems. When the working fluid is R1270, systems have the lowest power consumption.
- As the BOG content increases, the power consumption of both integrated systems and non-integrated systems increase. At different BOG contents, the power consumption of the integrated system is less than its corresponding non-integrated system. And with the increase of BOG content, the power consumption reduction rate of the integrated system is gradually reduced. Among them, the two-stage reconcondensation process and LNG cold energy power generation integrated system has the largest reduction rate of power consumption. When the BOG content is 0.03, the power consumption reduction rate is 250%. When the BOG content is 0.15, the power reduction rate is 120%.

Acknowledgement

This research was financially supported by the National Natural Science Foundation of China (No. 51606025), MOST innovation team in key area (No. 2016RA4053) and the Fundamental Research Funds for the Central Universities (Grant No. DUT19JC05).

Nomenclature

W	output power (kW)
m	mass flow rate (kg/s)
η	isentropic efficiency (%)
h	specific enthalpy (kJ/kg)
P	pressure (kPa)
T	temperature (°C)

β BOG content from storage tank

Abbreviations

BOG	boil off gas
LNG	liquefied natural gas
NG	natural gas
ODP	ozone depression potential
GWP	global warming potential
Eva	evaporator
Con	condenser
SV	seawater vaporizer
R	recondenser

Subscripts

WF	working fluid
net	net power output
PC	power consumption
C	compressor
LP	low-pressure liquefied natural gas pump
MP	medium-pressure liquefied natural gas pump
HP	high-pressure liquefied natural gas pump
i	the number of compressor or pump

References

- Agarwal, R., Rainey, T., Rahman, S., Steinberg, T., Perrons, R., Brown, R., 2017. LNG regasification terminals: the role of geography and meteorology on technology choices. *Energies* 10 (12), 2152.
- Angelino, G., Invernizzi, C.M., 2011. The role of real gas Brayton cycles for the use of liquid natural gas physical exergy. *Appl. Therm. Eng.* 31 (5), 827–833.
- Atienza-Márquez, A., Bruno, J.C., Coronas, A., 2018. Cold recovery from LNG-regasification for polygeneration applications. *Appl. Therm. Eng.* 132, 463–478.
- Badami, M., Bruno, J.C., Coronas, A., Fambri, G., 2018. Analysis of different combined cycles and working fluids for LNG exergy recovery during regasification. *Energy* 159, 373–384.
- Bao, J., Lin, Y., Zhang, R., Zhang, N., He, G., 2017. Strengthening power generation efficiency utilizing liquefied natural gas cold energy by a novel two-stage condensation Rankine cycle (TCRC) system. *Energy Convers. Manag.* 143, 312–325.
- Bao, J., Zhang, R., Yuan, T., Zhang, X., Zhang, N., He, G., 2018. A simultaneous approach to optimize the component and composition of zeotropic mixture for power generation systems. *Energy Convers. Manag.* 165, 354–362.
- Boyaghchi, F.A., Sohbato, A., 2018. Assessment and optimization of a novel solar driven natural gas liquefaction based on cascade ORC integrated with linear Fresnel collectors. *Energy Convers. Manag.* 162, 77–89.
- Calm JM, H.G.P., 2011. Physical, safety, and environmental data for current and alternative refrigerants. In: The 23rd International Congress of Refrigeration.
- Dispenza, C., Dispenza, G., La Rocca, V., Panno, G., 2009. Exergy recovery during LNG regasification: electric energy production—Part one. *Appl. Therm. Eng.* 29 (2), 380–387.
- Dong, H., Zhao, L., Zhang, S., Wang, A., Cai, J., 2013. Using cryogenic exergy of liquefied natural gas for electricity production with the Stirling cycle. *Energy* 63, 10–18.
- Fernández-Polanco, D., Tatsumi, H., 2016. Optimum energy integration of thermal hydrolysis through pinch analysis. *Renew. Energy* 96, 1093–1102.
- Ferreira, P., Catarino, I., Vaz, D., 2017. Thermodynamic analysis for working fluids comparison in Rankine-type cycles exploiting the cryogenic exergy in Liquefied Natural Gas (LNG) regasification. *Appl. Therm. Eng.* 121, 887–896.
- Franco, A., Casarosa, C., 2015. Thermodynamic analysis of direct expansion configurations for electricity production by LNG cold energy recovery. *Appl. Therm. Eng.* 78, 649–657.
- García, R.F., Carril, J.C., Gomez, J.R., Gomez, M.R., 2016. Combined cascaded Rankine and direct expander based power units using LNG (liquefied natural gas) cold as heat sink in LNG regasification. *Energy* 105, 16–24.
- Ghaebi, H., Namin, A.S., Rostamzadeh, H., 2018. Exergoeconomic optimization of a novel cascade Kalina/Kalina cycle using geothermal heat source and LNG cold energy recovery. *J. Clean. Prod.* 189, 279–296.
- Gómez, M.R., García, R.F., Gómez, J.R., Carril, J.C., 2014. Review of thermal cycles exploiting the exergy of liquefied natural gas in the regasification process. *Renew. Sustain. Energy Rev.* 38, 781–795.
- Hasan, M.M.F., Zheng, A.M., Karimi*, I.A., 2009. Minimizing boil-off losses in liquefied natural gas transportation. *Ind. Eng. Chem. Res.* 48, 9571–9580.
- He, S.N., Chang, H.W., Zhang, X.Q., Shu, S.M., Duan, C., 2015. Working fluid selection for an Organic Rankine Cycle utilizing high and low temperature energy of an LNG engine. *Appl. Therm. Eng.* 90, 579–589.
- Hongtan, L., Lixin, Y., 1999. Characteristics and applications of the cold heat exergy of liquid natural gas. *Energy Convers. Manag.* 40, 1515–1525.
- Kanbur, B.B., Xiang, L., Dubey, S., Choo, F.H., Duan, F., 2018. Mitigation of carbon dioxide emission using liquefied natural gas cold energy in small scale power generation systems. *J. Clean. Prod.* 200, 982–995.
- Karimi, I.A., Khan, M.S., 2018. Special issue on PSE advances in natural gas value chain. *Ind. Eng. Chem. Res.* 57, 5733–5735.
- Kemp, I.C., 2007. *Pinch Analysis and Process Integration* 2Ed. Butterworth-Heinemann, Oxford.
- Le, S., Lee, J.-Y., Chen, C.-L., 2018. Waste cold energy recovery from liquefied natural gas (LNG) regasification including pressure and thermal energy. *Energy* 152, 770–787.
- Lee, S., 2017. Multi-parameter optimization of cold energy recovery in cascade Rankine cycle for LNG regasification using genetic algorithm. *Energy* 118, 776–782.
- Lee, H.Y., Kim, K.H., 2015. Energy and exergy analyses of a combined power cycle using the organic rankine cycle and the cold energy of liquefied natural gas. *Entropy* 17 (9), 6412–6432.
- Lee, U., Kim, K., Han, C., 2014. Design and optimization of multi-component organic rankine cycle using liquefied natural gas cryogenic exergy. *Energy* 77, 520–532.
- Li, Y., Wen, M., 2017. Boil-off gas two-stage compression and recondensation process at a liquefied natural gas receiving terminal. *Chem. Eng. Res. Des.* 40 (1), 18–27.
- Li, Y., Chen, X., Chein, M.-H., 2012. Flexible and cost-effective optimization of BOG (boil-off gas) recondensation process at LNG receiving terminals. *Chem. Eng. Res. Des.* 90 (10), 1500–1505.
- Li, P.C., Li, J., Pei, G., Munir, A., Ji, J., 2016. A cascade organic Rankine cycle power generation system using hybrid solar energy and liquefied natural gas. *Sol. Energy* 127, 136–146.
- Liu, C., Zhang, J., Xu, Q., Gossage, J.L., 2010. Thermodynamic-analysis-based design and operation for boil-off gas flare minimization at LNG receiving terminals. *Ind. Eng. Chem. Res.* 49 (16), 7412–7420.
- Lu, T., Wang, K.S., 2009. Analysis and optimization of a cascading power cycle with liquefied natural gas (LNG) cold energy recovery. *Appl. Therm. Eng.* 29 (8–9), 1478–1484.
- Mallapragada, D.S., Reyes-Bastida, E., Roberto, F., McElroy, E.M., Veskovic, D., Laurenzi, I.J., 2018. Life cycle greenhouse gas emissions and freshwater consumption of liquefied Marcellus shale gas used for international power generation. *J. Clean. Prod.* 205, 672–680.
- Manizadeh, A., Entezari, A., Ahmadi, R., 2018. The energy and economic target optimization of a naphtha production unit by implementing energy pinch technology. *Case Stud. Therm. Eng.* 12, 396–404.
- Mehrpooya, M., Sharifzadeh, M.M.M., Rosen, M.A., 2016. Energy and exergy analyses of a novel power cycle using the cold of LNG (liquefied natural gas) and low-temperature solar energy. *Energy* 95, 324–345.
- Mehrpooya, M., Esfilar, R., Moosavian, S.A., 2017. Introducing a novel air separation process based on cold energy recovery of LNG integrated with coal gasification, transcritical carbon dioxide power cycle and cryogenic CO₂ capture. *J. Clean. Prod.* 142, 1749–1764.
- Mehrpooya, M., Sharifzadeh, M.M.M., Katooli, M.H., 2018. Thermodynamic analysis of integrated LNG regasification process configurations. *Prog. Energy Combust. Sci.* 69, 1–27.
- Messineo, A., Panno, D., 2008. Potential applications using LNG cold energy in Sicily. *Int. J. Energy Res.* 32 (11), 1058–1064.
- Mosaffa, A., Mokarram, N.H., Farshi, L.G., 2017. Thermo-economic analysis of combined different ORCs geothermal power plants and LNG cold energy. *Geothermics* 65, 113–125.
- Nagesh Rao, H., Karimi, I.A., 2018. Optimal design of boil-off gas reliquefaction process in LNG regasification terminals. *Comput. Chem. Eng.* 117, 171–190.
- Nemati, A., Nami, H., Yari, M., 2018. Assessment of different configurations of solar energy driven organic flash cycles (OFCs) via exergy and exergoeconomic methodologies. *Renew. Energy* 115, 1231–1248.
- Noh, Y., Kim, J., Kim, J., Chang, D., 2018. Economic evaluation of BOG management systems with LNG cold energy recovery in LNG import terminals considering quantitative assessment of equipment failures. *Appl. Therm. Eng.* 143, 1034–1045.
- Oliveti, G., Arcuri, N., Bruno, R., De Simone, M., 2012. A rational thermodynamic use of liquefied natural gas in a waste incinerator plant. *Appl. Therm. Eng.* 35, 134–144.
- Parikhani, T., Gholizadeh, T., Ghaebi, H., Sattari Sadat, S.M., Sarabi, M., 2019. Exergoeconomic optimization of a novel multigeneration system driven by geothermal heat source and liquefied natural gas cold energy recovery. *J. Clean. Prod.* 209, 550–571.
- Park, C., Lee, C.-J., Lim, Y., Lee, S., Han, C., 2010. Optimization of recirculation operating in liquefied natural gas receiving terminal. *J. Taiwan Inst. Chem. E* 41 (4), 482–491.
- Pio, G., Salzano, E., 2019. The effect of ultra-low temperature on the flammability limits of a methane/air/diluent mixtures. *J. Hazard Mater.* 362, 224–229.
- Pospíšil, J., Charvát, P., Arsenyeva, O., Klimes, L., Špiláček, M., Klemes, J., 2019. Energy demand of liquefaction and regasification of natural gas and the potential of LNG for operative thermal energy storage. *Renew. Sustain. Energy Rev.* 99, 1–15.
- Querol, E., Gonzalez-Reguer, B., García-Torrent, J., García-Martínez, M., 2010. Boil off gas (BOG) management in Spanish liquid natural gas (LNG) terminals. *Appl. Energy* 87 (11), 3384–3392.
- Querol, E., Gonzalez-Reguer, B., García-Torrent, J., Ramos, A., 2011. Available power generation cycles to be coupled with the liquid natural gas (LNG) vaporization process in a Spanish LNG terminal. *Appl. Energy* 88, 2382–2390.

- Rao, W.J., Zhao, L.J., Liu, C., Zhang, M.G., 2013. A combined cycle utilizing LNG and low-temperature solar energy. *Appl. Therm. Eng.* 60 (1–2), 51–60.
- Rao, H.N., Wong, K.H., Karimi, I.A., 2016. Minimizing power consumption related to BOG reliquefaction in an LNG regasification terminal. *Ind. Eng. Chem. Res.* 55 (27), 7431–7445.
- Renzi, M., Brandoni, C., 2014. Study and application of a regenerative Stirling cogeneration device based on biomass combustion. *Appl. Therm. Eng.* 67 (1–2), 341–351.
- Rovira, A., Muñoz-Antón, J., Montes, M.J., Martínez-Val, J.M., 2013. Optimization of Brayton cycles for low-to-moderate grade thermal energy sources. *Energy* 55, 403–416.
- S. Sadaghiani, M., Ahmadi, M.H., Mehrpooya, M., Pourfayaz, F., Feidt, M., 2018. Process development and thermodynamic analysis of a novel power generation plant driven by geothermal energy with liquefied natural gas as its heat sink. *Appl. Therm. Eng.* 133, 645–658.
- Sadreddini, A., Ashjari, M.A., Fani, M., Mohammadi, A., 2018. Thermodynamic analysis of a new cascade ORC and transcritical CO₂ cycle to recover energy from medium temperature heat source and liquefied natural gas. *Energy Convers. Manag.* 167, 9–20.
- Salimpour, M.R., Zahedi, M.A., 2012. Proposing a novel combined cycle for optimal exergy recovery of liquefied natural gas. *Heat Mass Transf.* 48 (8), 1309–1317.
- Shi, J., Li, T., Peng, S., Liu, Z., Zhang, H., Jiang, Q., 2015. Comparative Life Cycle Assessment of remanufactured liquefied natural gas and diesel engines in China. *J. Clean. Prod.* 101, 129–136.
- Shin, M.W., Shin, D., Choi, S.H., Yoon, E.S., Han, C., 2007. Optimization of the operation of boil-off gas compressors at a liquefied natural gas gasification plant. *Ind. Eng. Chem. Res.* 46 (20), 6540–6545.
- Smith, R., 2005. *Chemical Process Design and Integration*. John Wiley.
- Soffiato, M., Frangopoulos, C.A., Manente, G., Rech, S., Lazzaretto, A., 2015. Design optimization of ORC systems for waste heat recovery on board a LNG carrier. *Energy Convers. Manag.* 92, 523–534.
- Song, R., Cui, M., Liu, J., 2017. Single and multiple objective optimization of a natural gas liquefaction process. *Energy* 124, 19–28.
- Souifi, M., Souissi, A., 2019. Simultaneous water and energy saving in cooling water networks using pinch approach. *Mater. Today: Proceedings* 13, 1115–1124.
- Sun, Z., Lai, J., Wang, S., Wang, T., 2018. Thermodynamic optimization and comparative study of different ORC configurations utilizing the exergies of LNG and low grade heat of different temperatures. *Energy* 147, 688–700.
- Sung, T., Kim, K.C., 2016. Thermodynamic analysis of a novel dual-loop organic Rankine cycle for engine waste heat and LNG cold. *Appl. Therm. Eng.* 100, 1031–1041.
- Tomkow, L., Cholewinski, M., 2015. Improvement of the LNG (liquid natural gas) regasification efficiency by utilizing the cold exergy with a coupled absorption - ORC (organic Rankine cycle). *Energy* 87, 645–653.
- Tuinier, M.J., van Sint Annaland, M., Kramer, G.J., Kuipers, J.A.M., 2010. Cryogenic CO₂ capture using dynamically operated packed beds. *Chem. Eng. Sci.* 65 (1), 114–119.
- Wang, G.-B., Zhang, X.-R., 2017. Thermodynamic analysis of a novel pumped thermal energy storage system utilizing ambient thermal energy and LNG cold energy. *Energy Convers. Manag.* 148, 1248–1264.
- Williams, P.M., Ahmad, M., Connolly, B.S., Oatley-Radcliffe, D.L., 2015. Technology for freeze concentration in the desalination industry. *Desalination* 356, 314–327.
- Wu, M., Zhu, Z., Sun, D., He, J., Tang, K., Hu, B., Tian, S., 2019. Optimization model and application for the recondensation process of boil-off gas in a liquefied natural gas receiving terminal. *Appl. Therm. Eng.* 147, 610–622.
- Xue, F., Chen, Y., Ju, Y., 2017. Design and optimization of a novel cryogenic Rankine power generation system employing binary and ternary mixtures as working fluids based on the cold exergy utilization of liquefied natural gas (LNG). *Energy* 138, 706–720.
- Zhang, M.-G., Zhao, L.-J., Liu, C., Cai, Y.-L., Xie, X.-M., 2016. A combined system utilizing LNG and low-temperature waste heat energy. *Appl. Therm. Eng.* 101, 525–536.
- Zhang, M.-G., Zhao, L.-J., Xiong, Z., 2017. Performance evaluation of organic Rankine cycle systems utilizing low grade energy at different temperature. *Energy* 127, 397–407.
- Zhang, H., Guan, X., Ding, Y., Liu, C., 2018. Emergy analysis of Organic Rankine Cycle (ORC) for waste heat power generation. *J. Clean. Prod.* 183, 1207–1215.